



<b>Publication Year</b>	2016
<b>Acceptance in OA</b>	2020-05-21T10:45:18Z
<b>Title</b>	New fully empirical calibrations for strong-line metallicity indicators in star forming galaxies
<b>Authors</b>	Curti, M., CRESCI, GIOVANNI, MANNUCCI, FILIPPO, Marconi, Alessandro, Maiolino, R., ESPOSITO, Simone
<b>Handle</b>	<a href="http://hdl.handle.net/20.500.12386/25039">http://hdl.handle.net/20.500.12386/25039</a>



# New fully empirical calibrations for strong-line metallicity indicators in star forming galaxies

M. Curti<sup>1,2</sup>, G. Cresci<sup>1</sup>, F. Mannucci<sup>1</sup>, A. Marconi<sup>2</sup>, R. Maiolino<sup>3,4</sup>, S. Esposito<sup>1</sup>

<sup>1</sup> INAF, Osservatorio Astrofisico di Arcetri <sup>2</sup> Università degli Studi di Firenze <sup>3</sup> Cavendish Laboratory, University of Cambridge <sup>4</sup> Kavli Institute for Cosmology, University of Cambridge



We derive new empirical calibrations for some of the most widely used strong-line diagnostics of gas phase metallicity in star forming galaxies, thanks to a uniform application of the Te method over the full metallicity range probed by the Sloan Digital Sky Survey. We stacked spectra of more than 110000 galaxies in bins of  $\log [\text{O II}]/\text{H}\beta - \log [\text{O III}]/\text{H}\beta$  in order to detect and measure the fluxes of the faint auroral lines needed to compute the electron temperatures and apply the Te method. Our calibrations are defined on a consistent absolute metallicity scale for galaxies, they span more than 1 dex in  $\log(\text{O}/\text{H})$  and provide metallicity estimates in agreement to within 0.05 dex. Compared to other studies (Andrews & Martini 2013; Brown et al. 2016), our approach does not assume any dependence of metallicity on mass and star formation rate, but rely only on the validity of the Strong Line Methods.

## Method

- Our goal is to obtain more consistent calibrations for the main strong-line metallicity indicators, thanks to a uniform application of the Te method.
- Since  $[\text{O II}]/\text{H}\beta$  and  $[\text{O III}]/\text{H}\beta$  are two common oxygen abundance diagnostics and are directly proportional to the main ionization states of oxygen, we assume that galaxies with similar values in both line ratios have approximately the same oxygen abundance.
- We then stacked spectra of SDSS galaxies in bins of 0.1 dex in the  $\log [\text{O II}]/\text{H}\beta - \log [\text{O III}]/\text{H}\beta$  diagram (Figure 1).
- We measured the electron temperature of the low ionization zone ( $T_2$ ) from the  $[\text{O II}] \lambda\lambda 7320, 7330/[\text{O II}] \lambda 3727$  diagnostic ratio and the electron temperature of the high ionization zone ( $T_3$ ) from the  $[\text{O III}] \lambda 4363/[\text{O III}] \lambda 5007$  diagnostic ratio or from the ff-relation (Pilyugin et al. 2006a) for stacks with undetected  $[\text{O III}] \lambda 4363$  (see Figure 3).
- We computed the  $\text{O}^+$  and  $\text{O}^{++}$  ionic abundances, assuming then  $\text{O}/\text{H} = \text{O}^+/\text{H}^+ + \text{O}^{++}/\text{H}^+$ .

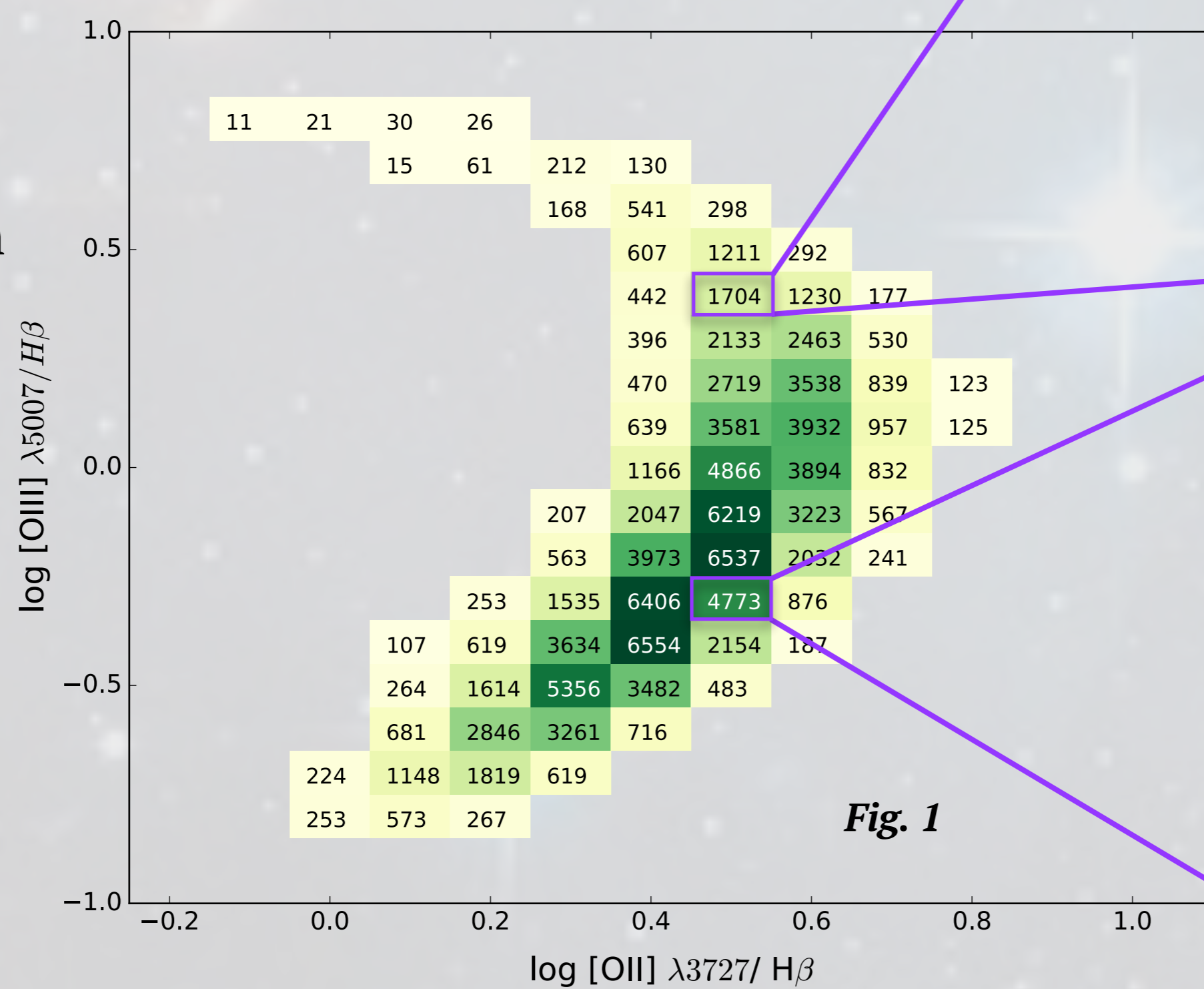


Fig. 1

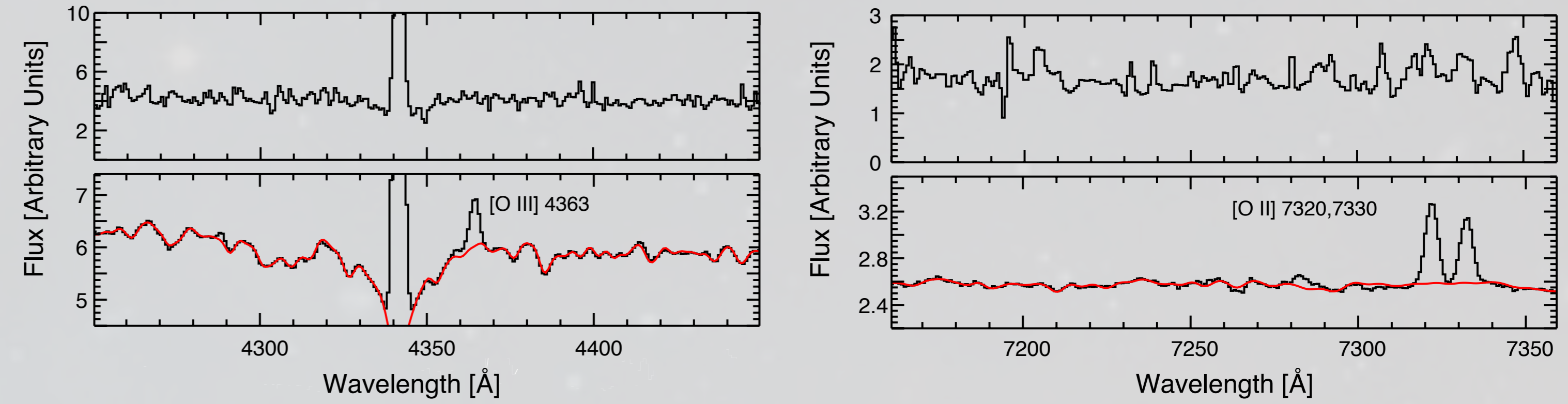


Fig. 2 : Comparison between a single galaxy spectrum (top) and a stacked spectrum (bottom) in the wavelength ranges of the  $[\text{O III}] \lambda 4363$  (left) and  $[\text{O II}] \lambda\lambda 7320, 7330$  (right) auroral lines. Auroral lines are easily detected in the stacked spectra. The red curve represents a fit to the stellar continuum.

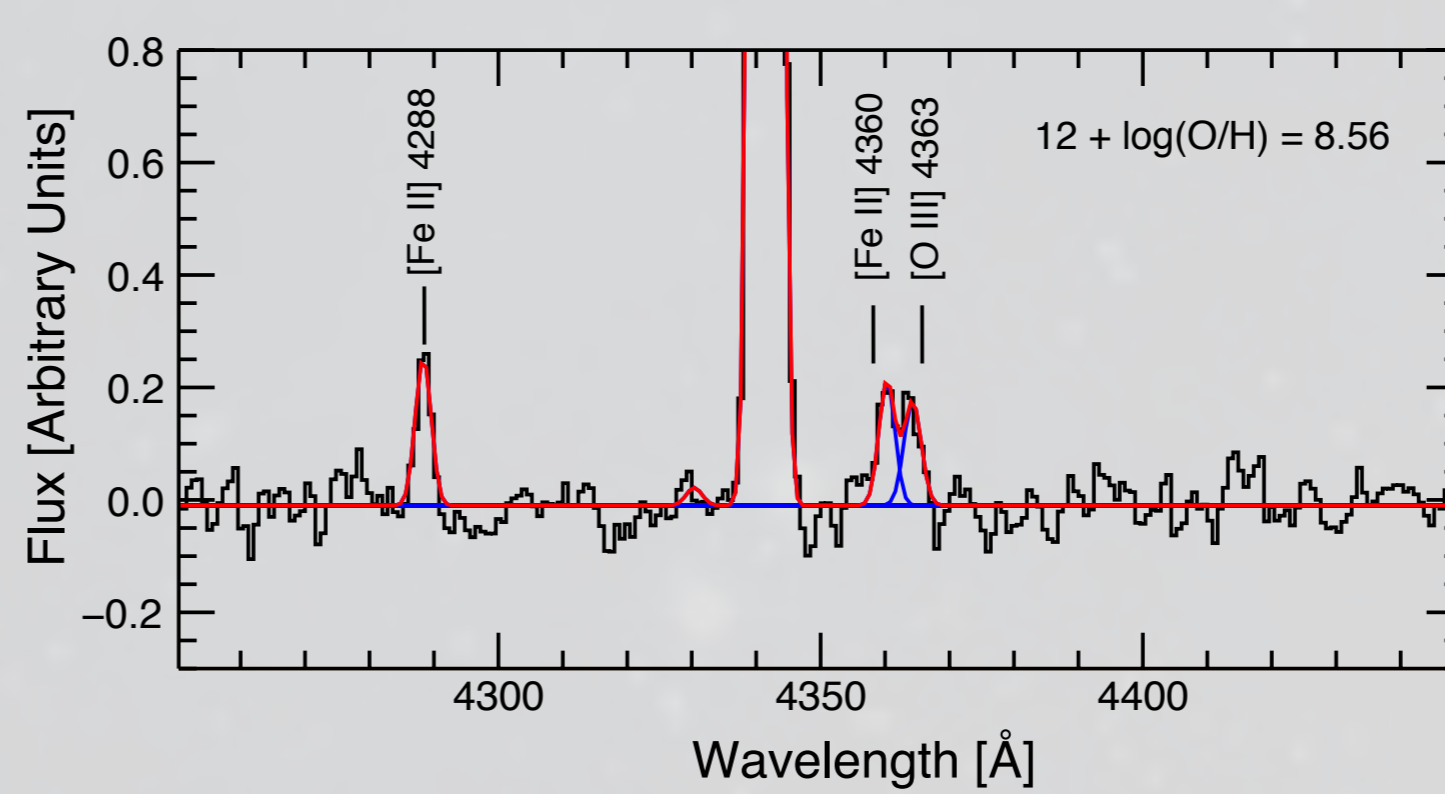


Fig. 3 : During the fitting procedure a spectral feature close to 4360 Å became blended with the  $[\text{O III}] \lambda 4363$  line in high metallicity stacks (see also Andrews & Martini 2013). This feature can be associated to emission from the  $\text{Fe}^+$  ion. Others features from the same ion are indeed detected both in the same ( $[\text{Fe II}] \lambda 4288$ ) and in different spectral windows. This prevents a robust measure of  $[\text{O III}] \lambda 4363$  flux in some of our stacks.

## Calibrations

- We re-calibrated the following indicators :  
 $R_3 = [\text{O III}] \lambda 5007/\text{H}\beta$   
 $R_{23} = ([\text{O III}] \lambda 5007 + [\text{O II}] \lambda 3727)/\text{H}\beta$   
 $N_2 = [\text{N II}] \lambda 6584/\text{H}\alpha$   
 $\text{O}_3\text{N}_2 = ([\text{O III}] \lambda 5007/\text{H}\beta)/([\text{N II}] \lambda 6584/\text{H}\alpha)$
- To extend the range covered by our calibrations, we included a sample of low metallicity galaxies with robust ( $>10\sigma$ ) detection of  $[\text{O III}] \lambda 4363$ .
- We define our new calibrations with a polynomial fitting, weighting each stack by the square root of the number of galaxies included in it.
- Dispersions in our calibrations are of the order of 0.10-0.15 dex
- Comparison with the semi-empirical calibrations from Maiolino et al. 2008 reveals how our calibrations deviate in the high metallicity regime, since Te method metallicities of our stacks result lower than those predicted by photoionization models.
- For the  $\text{O}_3\text{N}_2$  and  $\text{N}_2$  indicators we can compare our calibrations with the empirical ones from Pettini & Pagel 2004 and Marino et al. 2013. Our calibrations have comparable slopes but present a systematic offset towards higher metallicities, due to the fact that calibrations entirely based on HII regions samples are biased towards high excitation conditions and low metallicities.

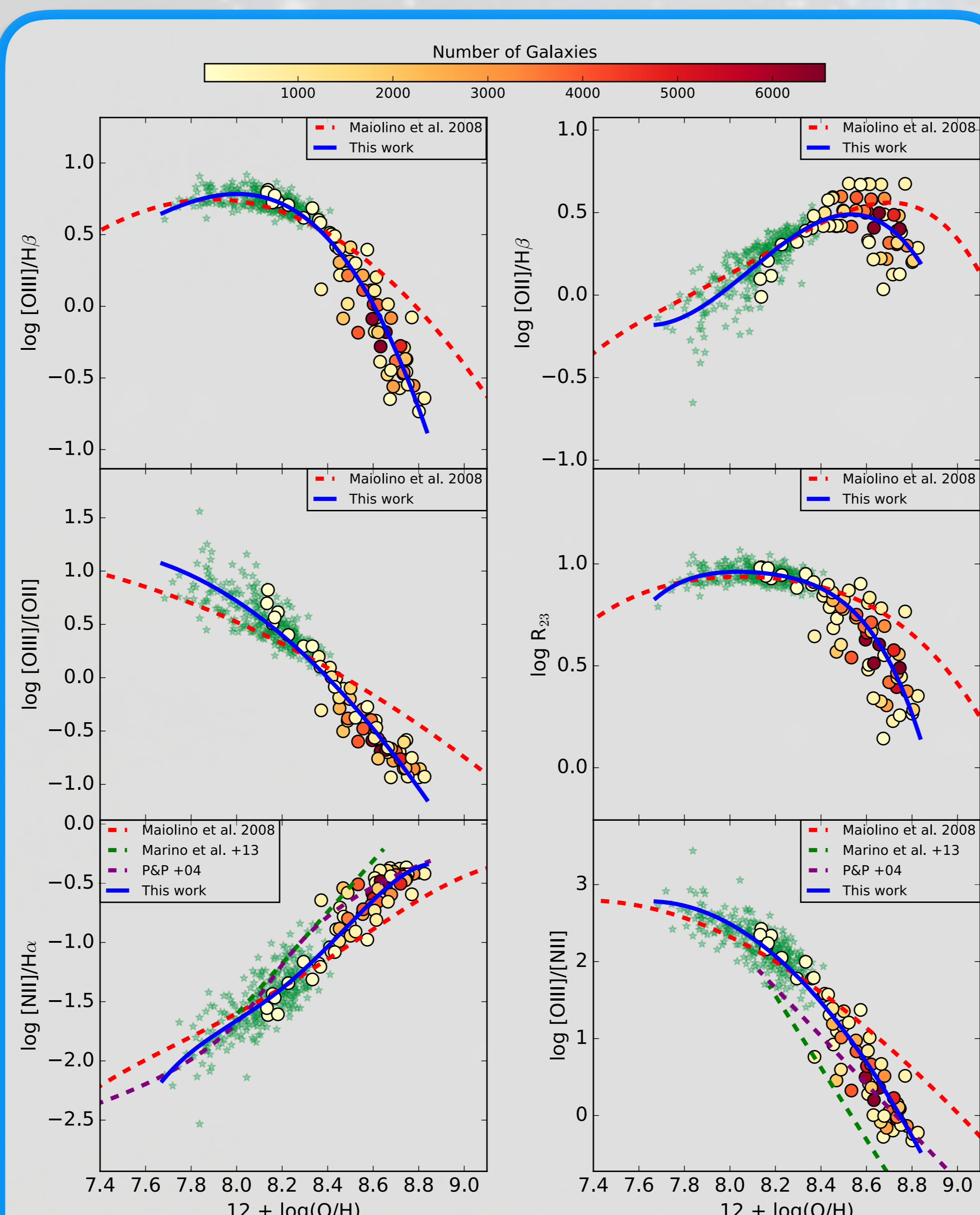


Fig. 4 : Strong Line diagnostics as a function of oxygen abundance for our full sample: small green stars represent the sample of single SDSS galaxies with  $[\text{O III}] \lambda 4363$  detection, while circles are the stacks color coded by the number of galaxies in each bin. Our best fit polynomial functions are shown as solid blue curves. Dashed lines are different calibrations from literature.

- We applied individually our new calibrations to the original sample of SDSS galaxies, finding good agreement between metallicities probed by different indicators.
- The average offsets are below 0.05 dex and typical dispersions in  $\Delta(\text{O}/\text{H})$  distributions are below 0.1 dex; our calibrations represent therefore a self consistent set.

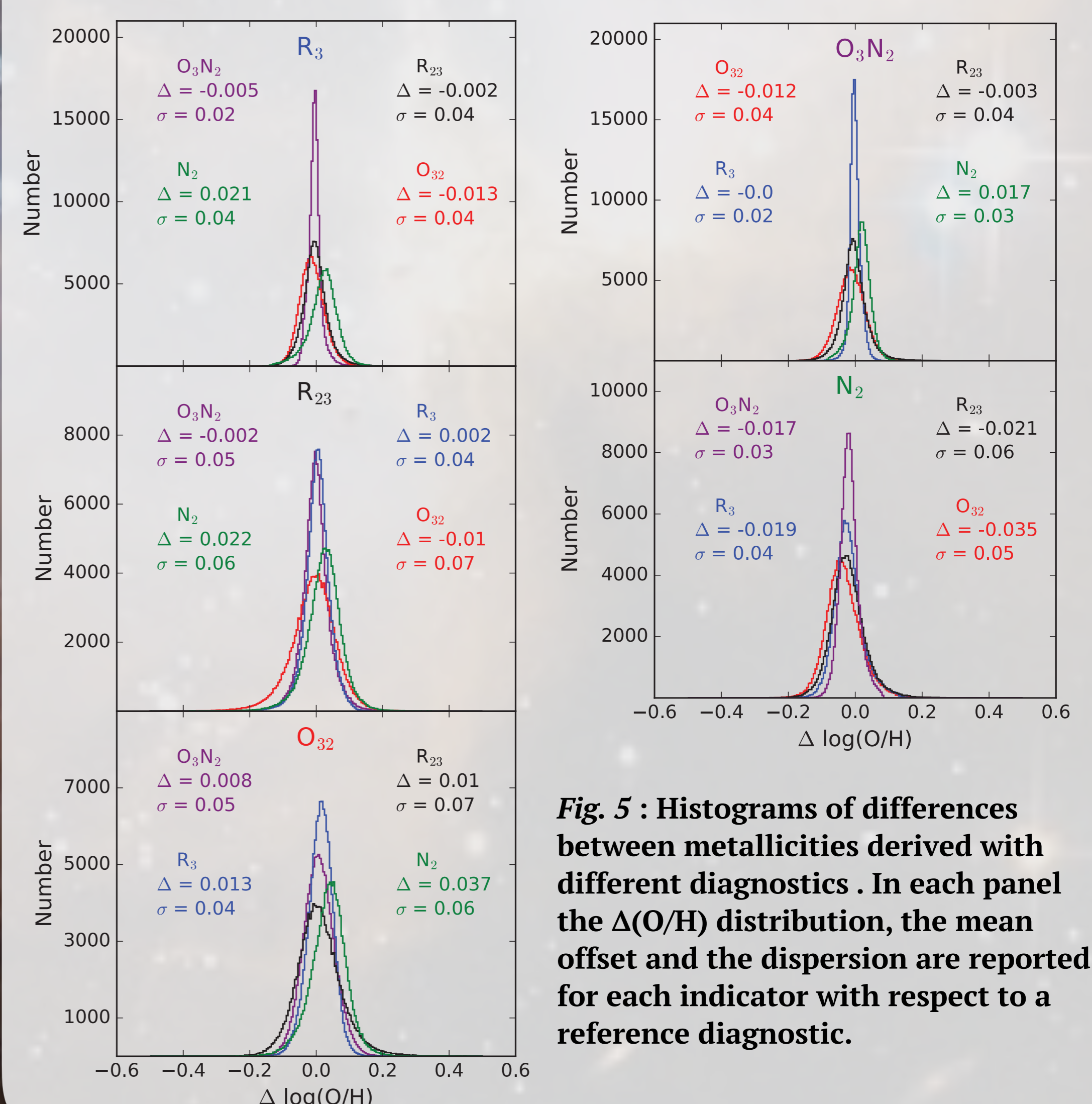


Fig. 5 : Histograms of differences between metallicities derived with different diagnostics . In each panel the  $\Delta(\text{O}/\text{H})$  distribution, the mean offset and the dispersion are reported for each indicator with respect to a reference diagnostic.

## References

Andrews B. H., Martini P., 2013, *AJ*, 146, 140  
 Brown J. S., Martini P., Andrews B. H., 2016, preprint, (arXiv:1602.01087)  
 Maiolino R., et al., 2008, *A&A*, 488, 463  
 Marino R. A., et al., 2013, *A&A*, 559, A114  
 Pettini M., Pagel B. E. J., 2004, *MNRAS*, 348, L59  
 Pilyugin L.S., Thuan T.X., Vilchez J.M., 2006a, *MNRAS*, 367, 1139